3-25 *IMPROVING DOPPLER VELOCITY COVERAGE ON THE WSR-88D BY USING LOW PRFS WITH 2DVDA*

Autumn Losey-Bailor*[1], W. David Zittel[1], and Zhongqi Jing[1,2]
[1]NEXRAD Radar Operations Center, Norman, Oklahoma
[2]Centuria Corporation, Norman, Oklahoma

1. INTRODUCTION

The National Weather Service's (NWS's) S-Band Weather Surveillance Radar – 1988 Doppler (WSR-88D) network is constrained by the "Doppler dilemma," which forces a lower Nyquist velocity when unambiguous range is increased. To deal with this, the WSR-88D features a variety of scanning strategies and Pulse Repetition Frequencies (PRFs) to handle different weather situations. The selection of PRFs can be dictated either automatically by a software task or manually by the user.

With the fielding of the operational software Build 18 in 2018 for the WSR-88D, the Radar Operations Center (ROC) in Norman, OK increased the number of precipitation PRFs from 5 to 7, ranging from PRFs 2 to 8. PRF 8 has the highest Nyquist velocity and shortest unambiguous range, while PRF 2 has the lowest Nyquist velocity and longest unambiguous range. Therefore, the paper refers to low PRFs and low Nyquist velocities interchangeably. Additionally, "low Nyquist" will henceforth be designated as "LN."

Leading up to Build 18, the WSR-88D's default velocity dealiasing scheme, the Two-Dimensional Velocity Dealiasing Algorithm (2DVDA), was evaluated for performance at LN velocities. The purpose of this paper is to demonstrate the weather scenarios at LN velocities that the 2DVDA can dealias successfully and those that present challenges, and ultimately whether using low PRFs is a viable strategy for improving Doppler coverage. Section 2 provides background; Section 3 discusses the testing process and results from initial work with artificially generated LN cases; Section 4 describes the convergence of evaluating real-time low PRF cases with evaluating 2DVDA enhancements intended for fielding in Build 19 in 2020 and results thereof; Section 5 illustrates case studies; finally, Section 6 presents conclusions and future work.

** Corresponding Author Address:* Autumn D. Losey-Bailor, Radar Operations Center, Norman, OK, 73069-8480; email: autumn.d.losey-bailor@noaa.gov

2. BACKGROUND

This section provides necessary context for the main work. First, NEXRAD's available PRFs are discussed in greater detail. Second, an historical overview of methods to improve Doppler velocity coverage is provided, with a focus on the modified Sachidananda-Zrnic (SZ-2) technique. Finally, an overview of the 2DVDA as fielded in Build 18 is given.

2.1 *NEXRAD PRF Information*

With Build 18, there are 8 PRFs available for operational Doppler scan use (see Table 1). The lowest PRF is reserved for use by Volume Coverage Pattern (VCP) 31, which uses a pulse length of 4.5 µs, shaded in grey. The other 7 PRFs (pulse length 1.57 µs) are all available for use by any other VCP. PRF 4 is the default PRF for nearly all VCPs. Currently, operators must manually select PRFs 2 and 3.

Note that the values given for unambiguous range, Nyquist velocity, and pulse repetition times in the table will differ slightly from what may be observed in the field. The true values depend on the radar's frequency within the 2700 – 3000 MHz band. Table 1 values are for the ROC's testbed radar KCRI, which transmits at ~2900 MHZ. The National Severe Storms Laboratory's testbed radar KOUN transmits at ~2700 MHz; its VN for PRF 8 is ~36 ms-1, while the VN for PRF 1 is ~12 ms-1.

Table 1: This table lists the PRFs used by the WSR-88D. The green-shaded rows are available for use by the precipitation mode VCPs. Shown are typical unambiguous ranges (RA), Nyquist velocities (VN), and Pulse Repetition Times (PRT) for KCRI.

PRF	R_A (km)	V_N (m s^{-1})	PRT (µs)
1	331.0	11.16	2240.0
2	187.0	20.05	1246.7
3	175.0	21.43	1166.7
4	162.0	23.15	1080.0
5	148.0	25.34	986.7
6	137.0	27.37	913.3
7	127.0	29.53	846.7
8	117.0	32.05	780.0

2.2 *Enhanced Echo Coverage Techniques*

As far back as 1994, the Next-Generation Radar (NEXRAD) Technical Advisory Committee prioritized the reduction of velocity data loss due to range folding on the WSR-88D. Three different techniques emerged as candidates. Two of them, phase coding and Staggered Pulse Repetition Time (SPRT) required new waveforms at the data processing level (the RDA), while the third, the Multi-PRF Dealiasing Algorithm (MPDA) required new velocity dealiasing code at the product generation level (RPG) and a new scanning strategy. The SPRT approach requires special clutter filtering, which until recently rendered it unsuitable for low elevation angles (Torres 2006). Although work continues on SPRT, it has not yet met data quality requirements for fielding. Meanwhile, the MPDA and its corresponding VCP 121 were fielded in 2004 (Conway et al. 1997). Though the extra scans at complementary PRFs provide reliable velocity estimates and improved coverage, the data collection time is slower and MPDA has found limited operational use. The phase coding approach, known as the Sachidananda/Zrnic (SZ 8/64) technique, was fielded in 2007 (Sachidananda et al. 1998).

In brief, SZ-2, a modified version of the Sachidananda/Zrnic (SZ 8/64) algorithm that includes a surveillance scan, is used to reduce range folding in conjunction with a high PRF to mitigate velocity dealiasing errors (Saxion et al. 2007). With a high PRF, microwave energy from previous pulses may be mixed with microwave energy from the current pulse. Energy from previous pulses is referred to as second trip echo, third trip echo, etc., while energy from the first trip pulse is referred to as first trip echo. By changing the phase of succeeding pulses and use of autocorrelation, SZ-2 can separate 1st trip from 2nd trip echo.

Although we retrieve more coverage with SZ-2 at higher PRFs, the range folding at the start of 2nd trip or even 3rd trip can obscure important weather features. If low PRFs can be reliably used, the 1st trip coverage can be maximized and the weather signal of greatest interest/significance preserved. Also, this minimizes the coverage of the weak (2nd trip) echo, which is prone to being noisy. Lastly, when using SZ-2 in higher PRFs, strong echoes from 3rd and even 4th trip can result in obscuration.

2.3 *The Two-Dimensional Velocity Dealiasing Algorithm*

The 2DVDA dealiases connected two-dimensional regions within an elevation scan by minimizing all detected velocity discontinuities. It calculates the difference between a gate and the neighboring gates, puts paired gates into a smoothness function, and applies a least squares method to find suitable velocity values that minimize the output of the smoothness function. To realize the full potential of the two-dimensional approach, the 2DVDA must be applied to a full elevation scan. This is done in two phases. In phase one, the full field is used to generate an internal environmental wind table. In order to conserve computer CPU and memory resources, the 2DVDA sub-samples large, complex fields. This is done by subsampling regions within the velocity field azimuthally and radially and computing a median velocity value for the center of each grid. In phase two, the 2DVDA partitions the elevation scan and then dealiases smaller features such as mesocyclones and tornado vortex signatures. Finally, the internally generated environmental wind table is used to place small, isolated regions in the correct Nyquist co-interval.

In the interest of increasing 2DVDA's robustness, a number of improvements have been added since its initial discussion in Jing and Wiener (1993). Most enhancements mentioned in Zittel and Jing (2012) are still in use: weighting velocity differences to reduce the contribution of noisy data to the optimization setting, separating regions connected by a narrow "bridge" of noisy data, and the temporary removal of sidelobe-contaminated data. Others have been removed once it was determined that they either harmed or did not contribute to the dealiasing solution, such as using spectrum width to help weight velocity differences. Since then, other enhancements have been added. These include: identifying and dealiasing region boundaries to predetermine the full region's aliased state, the addition of a gust front detection function to improve the quality of the background wind field, the addition of a simple storm base estimation algorithm to correct the data altitude in case of high vertical shear, using simple linear interpolation to improve the calculation of the vertical wind analysis portion of the 2DVDA's internal Velocity Azimuth Display (VAD) algorithm, a radial extrapolation method that provides better background wind for dealiasing remote hurricane cells, and saving a history of environmental and storm features. The most recent enhancements involve quality control methods for the internally developed VAD, such as computation of the Free Atmosphere Wind and greater allowance for the use of external model data (Losey et al. 2017).

Further updates have been made as a direct result of low-Nyquist testing. These updates will be discussed briefly in Section 4.1. The given overview of 2DVDA encompasses the algorithm as it was fielded in Build 18.

3. INITIAL TESTING AND RESULTS OF ARTIFICAL LOW-NYQUIST DATA

Testing dealiasing performance for LN velocities occurred in stages. The initial testing was conducted almost entirely without real-time LN data, since such data were not readily available. This section discusses how the data for the initial testing were created, gives an overview of the evaluation method and provides results, and finally, discusses how the results impacted later testing.

3.1 *Creating Artificial Velocity Data*

The authors frequently mention the dearth of true low-Nyquist data at the start of the evaluation. While this is true in a practical sense, there were several cases available that used VCP 31, whose Doppler PRF has a Nyquist velocity of 11 m/s. This VCP is typically used for clear air, winter weather, or slow, light precipitation – situations where features in reflectivity tend to take precedence over those in velocity. Velocity dealiasing results are generally poor in this VCP, especially during winter weather at the lowest elevation. While these types of cases provided a suggestion for the lowest Nyquist velocities to test, they were not otherwise useful for this part of the evaluation. Additionally, at Nyquist velocities lower than 15 ms^{-1}, the 2DVDA follows a slightly different logic path. Thus, with a lower boundary established in terms of the code, and an upper boundary with the Nyquist velocity of PRF 4, the range of velocity values to test ran from 15 to 21.4 ms^{-1}.

In order to find the effective performance limit in this range, data cases were created using an "artificial" Nyquist velocity. This was accomplished by taking an existing case and running it through a non-operational tool that took dealiased velocity data, re-aliased it, and then generated new data files with a new Nyquist velocity. The new data files were then processed through WSR-88D software and the performance evaluated. Due to the nature of the tool, cases with good dealiasing performance were chosen for testing. If a case had dealiasing errors originally, they would be refolded incorrectly and any true errors would be compounded or potentially masked. Another important factor about the tool was that it only affected velocity data – although the data were given a new "Nyquist" velocity, the actual PRF could not be changed, and so the unambiguous range did not change.

Cases were also selected that were likely to stress the 2DVDA once it was trying to process the refolded LN data. Therefore, most of the artificial cases are severe wind events, such as derechos or strong mesocyclones. A few less extreme cases were selected as a control group.

Because the initial goal was to find 2DVDA's performance limit, the testing method was straightforward. The case with its original Nyquist velocity was run to generate both a baseline and the new data with a new Nyquist velocity. The same data set was run with several different Nyquist velocities; the dealiasing results were then visually compared to the baseline. The runs at 20 ms^{-1} from this phase of testing showed the most promise and underwent more rigorous evaluation.

3.2 *Evaluation Method*

Dealiasing results from the original Nyquist data set were subjectively compared to results from the artificial LN set. Performance scores were based on the size and frequency of perceived errors. In the following discussions, the terms scan or cut are used interchangeably to reference one full 360° sweep at one elevation.

Each velocity image was subjectively assigned a score from 0 to 3 or 10. (The score jumps to 10 to indicate extreme outliers.) A score of 0 indicates that all important meteorological features are preserved and any range bins inconsistent with the expected solution are isolated, few in number (fewer than 20 bins), or nonexistent. Images scored as 1 show scattered bins that do not fit the expected pattern, but do not interfere with interpreting important meteorological features such as a mesocyclone or tornado vortex signature. Score 2 indicates small patches that are incorrectly dealiased (less than 25 km^2). Though distracting, these patches typically do not detract from correctly interpreting important features. A score of 3, however, indicates that large dealiasing errors severely impacted the recognition of important meteorological signatures. Finally, a score of 10 indicates dealiasing errors that interfere with understanding the basic flow or identification of zero-isodops. These last were very rare, and with one or two exceptions occurred only during the VCP 31 cases in later stages of testing. These cases are not part of this study. Figure1 shows an example of each score and Table 2 gives a summary of the score descriptions.

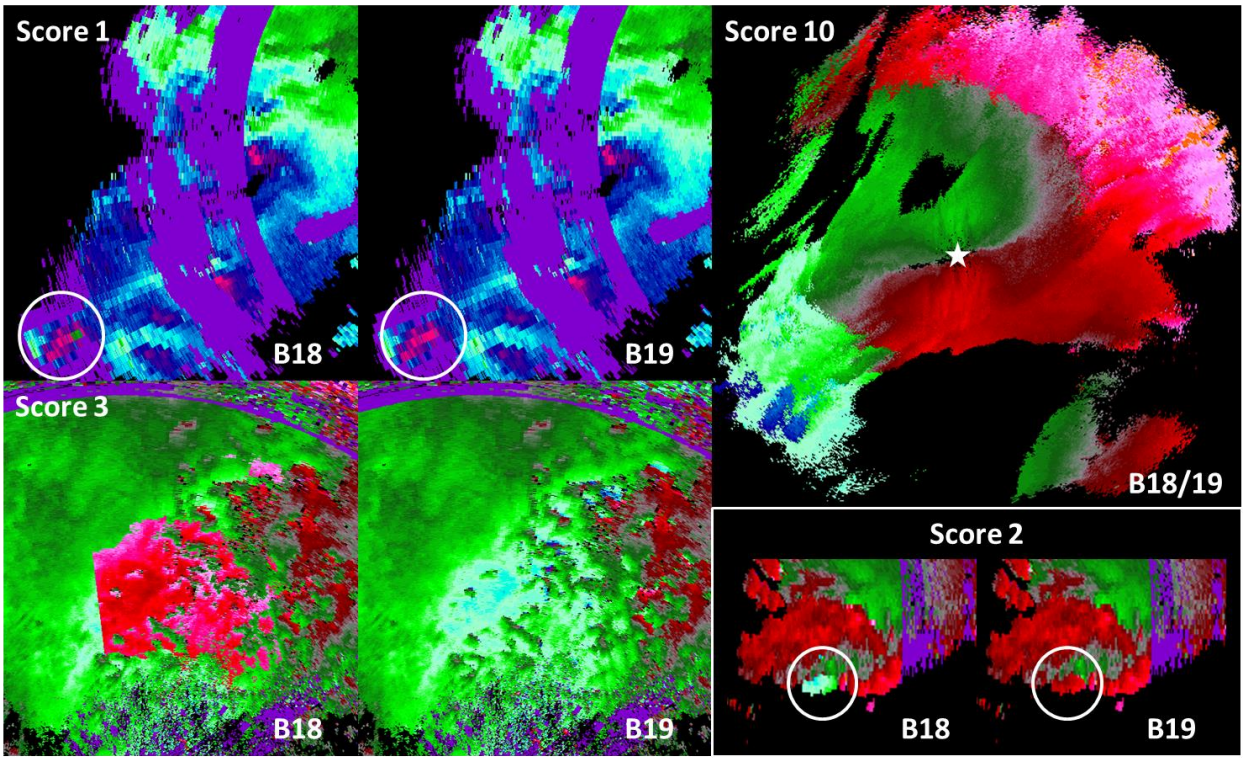

Figure 1: Visual representation of scores. This figure gives visual examples of the subjective scoring. For Scores 1-3, Build 18 has the error and Build 19 is clean (and would therefore represent a 0 score). This was done to clearly illustrate the error. The image for Score 10 is functionally the same for Builds 18 and 19. The star indicates the radar position. The cases shown are: Score 1 – KHTX 2011.27.04, Score 2 – KGGW 2018.21.07, Score 3 – KAMA 2018.25.06, and Score 10 – KDMX 2008.03.12. The KDMX case is a VCP 31 case, with a Nyquist velocity of 11 ms^{-1}.

Figure 1 also demonstrates some of the nuances in the scoring. For instance, in Score 1, the most noticeable error is circled in white. Many errors categorized as '1' are most noticeable during comparison and can provide insight into how 2DVDA accounts for single-bin oddities. The Score 2 example is also interesting. The error size itself is, in terms of bins, small enough to be considered a 1; however, the placement of the error and its size relative to the rest of the echo elevated its severity to 2. There were many subtleties to account for in scoring, but there also many straightforward examples. Scores 3 and 10 were quite blatant. Generally, interference from other radars, clutter contamination from windfarms, and other oddities from non-meteorological artifacts were ignored. Occasionally, noisy results from weak trip returns would increase a score, especially if the noise could be mistaken for important features.

Table 2: This table provides a brief description of scores assigned to each velocity image based on the subjective evaluation of the quality of the dealiased field.

Score	Description
0	No obvious errors in the dealiased velocity image
1	Isolated bins incorrectly dealiased that do not affect interpretation of the velocity image
2	Small patches with obvious dealiasing errors but do not affect important velocity features or signatures
3	Patches that interfere with recognition of important meteorological signatures
10	Large-scale errors that interfere with correct understanding of the velocity field, especially correct placement of 0 isodops

For each case, all elevation angles at or below 1.5° consisting of a surveillance scan (unambiguous range 460 km) followed by a Doppler scan using a PRF as defined in table 1. These are known as split cuts. Furthermore, to capture examples from every type of scan

in the volume, elevation angle 1.8° and the first elevation above 6.4° were also scored. The former corresponds to the first Batch cut, wherein a short burst of surveillance pulses is followed by a larger number of Doppler pulses in the same radial. The latter corresponds to the first Contiguous Doppler cut, which uses Doppler cuts to provide velocity and reflectivity. Additionally, some cases make use of Supplemental Adaptive Intravolume Low-level Scans (SAILS; Daniel et al. 2014), which in brief is an extra 0.5° cut repeated up to 3 times within a volume. This is why some cases with similar numbers of volumes have disparate numbers of cuts.

Once these scores were recorded, a weighted average was computed based on the number of instances of each score multiplied by the value of the score itself, summed, and divided by the total number of elevation cuts scored. This weighted average became the basis for statistical scoring.

3.3 *Results from Dealiasing Artificially Re-Aliased Data*

This phase of testing used sixteen individual data sets re-aliased to Nyquist velocities of 20 ms^{-1} or, in two instances, 15 ms^{-1}. The two 15 ms^{-1} cases were initially run at 20 ms^{-1}, but the source scientist requested those at the lower re-aliased Nyquist to assist with development for 2DVDA enhancements. This enhancement is discussed in greater detail in Section 4.

With their original Nyquist velocities, these cases were generally error-free when run with the Build 18 baseline 2DVDA. Table 3 summarizes the results. Values above 0.75 indicate cases with errors large and frequent enough to detract from correct operator interpretation. Values at or below 0.15 indicate cases with minimal error.

Table 3: This table shows the average dealiasing error for the 16 artificial low-Nyquist cases ranked from highest to lowest error. Note the higher scores of the two 15 ms^{-1} cases. The cases above 0.15 all feature mesocyclones and/or tornadoes, which suggested early on where LN problems would occur. The cases less than 0.15 in average error had severe winds or light convection moving in from a distance. These cases scored best.

Site	Date (dd.mm.yyyy)	# Vol	# Scans	Avg. Err. B18
KOAX	17.06.2017	16	110	1.47
KUDX	20.06.2015	22	132	1.17
KHTX	27.04.2011	30	145	1.01
KBMX	27.04.2011	27	135	0.85
KTLX	10.05.2010	15	75	0.60
KTLX	31.05.2013	28	140	0.59
KDVN	14.10.2017	19	130	0.57
KLSX	01.03.2017	21	128	0.40
KICT	12.06.2008	40	181	0.28
KTLX	20.05.2013	28	140	0.24
KILN	29.06.2012	27	135	0.17
KTLH	17.01.2016	20	82	0.06
KUEX	29.06.2016	31	166	0.06
KDDC	16.05.2015	19	130	0.04
KFCX	30.06.2012	13	65	0.03
KFSD	07.08.2015	28	65	0.00

It can be seen that the cases with most error are the two 15 ms^{-1} cases, which was expected. The cases with the greatest error all feature strong mesocyclones, supercells, and tornadoes – except one, the KDVN case, which was a squall line with strong shear. Ultimately, with the artificial LN data, it was very difficult to quantify why cases similar in nature scored so differently. The KFCX case, for example, is relatively similar to the KOAX case in terms of general environment; however, it experienced very minor errors. Also, it is possible that differences in rounding and truncation that occurred during the re-aliasing process introduced isolated errors. In spite of these caveats, there was enough of a trend to show that 2DVDA would have difficulty dealiasing mesocyclones at LN velocities. This result was anticipated, and the general thought was that a LN PRF would be a less likely candidate for forecasters to choose during those extreme weather events.

This initial testing helped establish general expectations for performance at lower Nyquist velocities – results seemed to deteriorate rapidly below 20 ms^{-1}, and in some instances were sub-par even at 20 ms^{-1}. However, there were some surprisingly good results as well, and the ROC decided to release the new LN PRFs with Build 18 so that real-time data could be obtained for further testing.

4. TESTING AND EVALUATION OF REAL-TIME LOW NYQUIST DATA

This stage of testing occurred once Build 18 was deployed with the new low PRFs as listed in Table 1. Even so, two factors made the availability of real-time low PRF data initially uncertain. First, PRFs 2 and 3 were only available for manual selection by the forecasters, who tend to favor the automatic PRF selection algorithm. The new default PRF for the algorithm became PRF 4. Second, the field received training about the pros and cons of the low PRFs – increased range at the cost of the potential for increased dealiasing errors.

Surprisingly, more sites chose to experiment with the new low PRFs than expected. This section discusses the subsequent refinement of the conclusions reached from initial testing. It also discusses the concurrent development and testing of 2DVDA enhancements designed to better handle LN velocities, especially in certain shear environments.

4.1 *Overview of 2DVDA Enhancement – The Nyquist Interval Map*

The Nyquist Interval (NI) map is meant to improve 2DVDA's performance in LNs while increasing its overall robustness in regards to quality control and specific types of shear handling. A known problem with LN velocities, as mentioned, is high shear. Shear that nears or exceeds the Nyquist co-interval can lead to dealiasing failures in 2DVDA specifically because the 2D algorithm that gives 2DVDA its name is unable to differentiate between borders of shear and borders of true aliasing. Smaller shear features, such as tornadoes, do not typically cause problems; large features and features along the edge of available data are most likely to fail. Knowing how these areas are aliased – i.e., determining the Nyquist interval of the region – adds additional information to the optimization equation for 2D dealiasing. This is the function of the NI map.

The NI map is a 2-dimensional map of the entire elevation cut, representing the data in terms of connected NI regions. Within each region, gates have the same Nyquist co-interval. Furthermore, the NI map is optimized to better handle specific "high local wind" shear features. This refers to either high shear lines (high gate-to-gate shear along the azimuth) or near-edge, high outbound winds (strong, local outbound wind near the edge of the data).

Though initially planned for Build 20, both need and promising results strongly encouraged fielding the NI map in Build 19. However, "promising" is not "perfect," and some issues remain.

4.2 *Evaluation Results – Build 18 vs. Build 19*

The evaluation method for the real-time LN cases is nearly identical to what is described in Section 3.2. The same scoring method summarized in Table 2 was used for this evaluation for consistency. Because the NI map enhancement constituted a major change for the 2DVDA, extensive testing was done to ensure that the new code did no harm to expected dealiasing solutions. Build 18 and 19 dealiasing results were compared visually and statistically to verify the performance of the enhanced 2DVDA in Build 19. A total of 42 cases, about 89 hours of data, were scored, 10 of which were from the original artificial Nyquist set of 16. Over the time frame of the testing, 7 real-time LN data sets were accumulated, 3 of which came from the field as error reports. Results from the 17 LN cases – real and artificial – are presented in Table 4 and further illustrated by Figure 2. These cases account for 32.5 hours of the full comparative data set.

Table 4 includes the average error for Build 19 and the difference in error between Builds 18 and 19. Difference values between -0.1 to 0.1 suggest that both builds essentially found the same dealiasing solutions. Values greater/less than +/-0.25 suggest strong improvement/degradation, respectively.

Table 4: Average dealiasing error for 2DVDA in Builds 18 and 19 for 17 LN (15 ms^{-1} - 20 ms^{-1}) data cases. The cases with * are the artificial LN cases; cases with ** are the 15 ms^{-1} cases. The data are sorted by the difference between Build 18 and 19; positive differences indicate improvement with Build 19, while negative differences indicate degradation. Overall, the NI map enhancement with Build 19 handled LN situations well, with no average error greater than 0.45.

				Avg. Err.		
Site	Date (dd.mm.yyyy)	# Vol	# Scans	Build 18	Build 19	Difference (B18 – B19)
KOAX**	17.06.2017	16	110	1.47	0.12	1.35
KUDX**	20.06.2015	22	132	1.17	0.24	0.93
KDVN*	14.10.2017	19	130	0.57	0.08	0.48
KLZK	20.02.2019	20	100	0.86	0.42	0.44
KAMA	25.06.2018	34	238	0.53	0.22	0.30
KTLX*	10.05.2010	15	75	0.60	0.39	0.21
KTLX*	31.05.2013	28	140	0.59	0.45	0.14
KTLX*	20.05.2013	28	140	0.24	0.13	0.11
KGGW	10.07.2018	24	136	0.46	0.38	0.09
KFDR	13.03.2019	12	67	0.16	0.13	0.03
KGGW	21.07.2018	34	232	0.16	0.14	0.01
KUEX*	29.06.2016	31	166	0.06	0.05	0.01
KTLH*	17.01.2016	20	82	0.06	0.07	-0.01
KTLX	13.03.2019	28	168	0.01	0.04	-0.03
KFCX*	20.06.2012	13	65	0.03	0.06	-0.03
KLBB	13.03.2019	24	132	0.01	0.05	-0.04
KFSD*	07.08.2015	28	65	0.00	0.06	-0.06

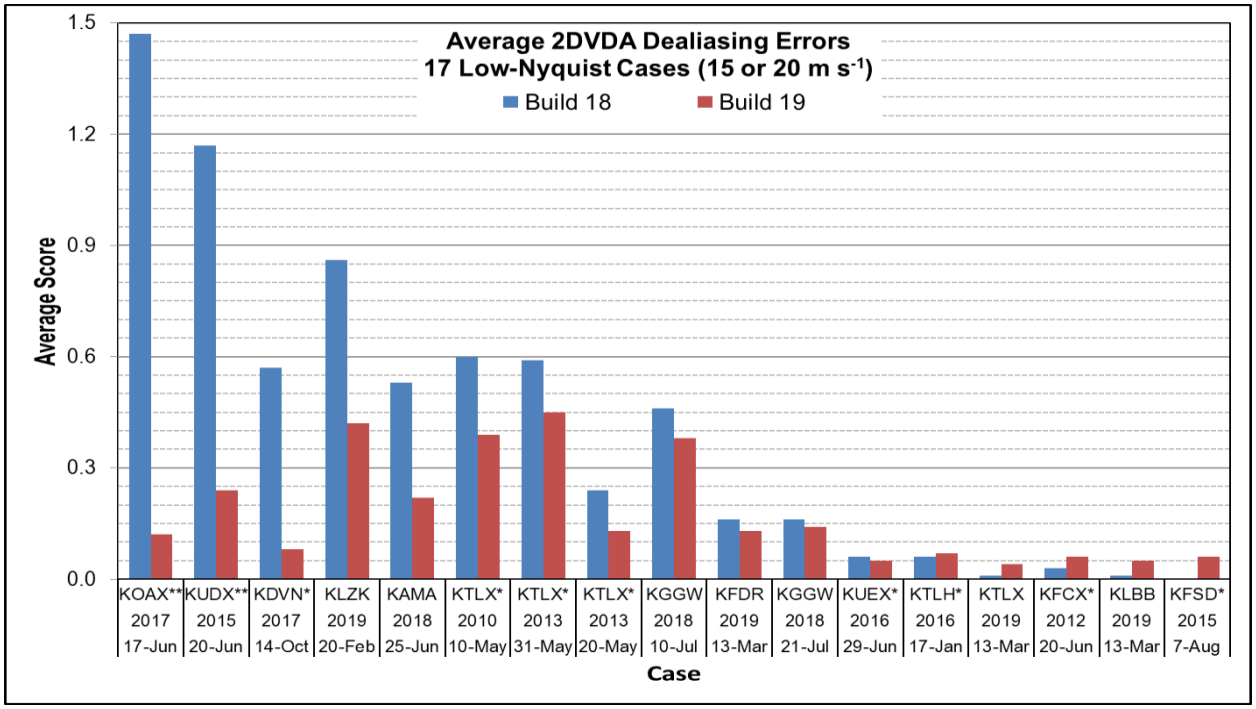

Figure 2: Average 2DVDA dealiasing errors for the 17 low Nyquist cases, using both artificial and real data, from Builds 18 and 19. Cases with * are the artificial low Nyquist cases; cases with ** are the 15 ms^{-1} cases. These are arranged from the highest to lowest difference between Build 18's average error, in blue, and Build 19's average error, in red. See Table 4 for exact values. Note that very few Build 19 errors reach beyond 0.3 in error, and that most fall below 0.15. Also note the last 5 cases, where Build 18 outperforms Build 19, and the cases that do exceed 0.3 in error.

Evaluated by its own average error, Build 19 performs well. The average error of the majority of cases in Build 19, for both the full comparative case set and the LN subset, fell between 0 and 0.15, which means that the cases did not show significant error. As seen in Table 4, the highest average error is 0.45 for one of the artificial cases featuring tornadic storms. The case with the next largest error at 0.42, KLZK, is one of the real-time PRF 2 cases and is further discussed in Section 5.

In terms of the code evaluation, Build 19 performs well compared to Build 18. For the full case set, the majority of cases fell between -0.1 to 0.1, which confirms that the enhanced code was not introducing new errors or exacerbating existing errors. For the LN cases, 7 of 17 cases show clear improvement in Build 19 over 18. Ten cases are within the minor difference range, though 5 of those are below 0.0. Some of this could be due to the subjective nature of the scoring, though some increased error is attributed to small differences in 2DVDA's clutter handling in the enhanced version causing some isolated bins to flip from one dealiased cointerval to the other. While the largely neutral results for the full case set were expected, the fact that the LN subset mirrors that result was surprising. The results for the LN subset suggest that, overall, the addition of the NI map is sufficiently successful, at least for the weather featured in the test cases.

Analysis of the differences also reveals types of cases that are still challenging with LN. However, understanding the complete mechanisms behind why those cases are more challenging proved difficult. While investigating cases from the testing data set provided insight, pertinent cases occurred after testing had concluded that narrowed down the causes of the remaining problems. Two of these cases, KDLH and KEAX, are discussed below in Section 5.

5. CASE STUDIES

This section presents 12 specific case studies that illustrate potentially difficult shear environments and how each was handled. The 1st case from 2017 shows an early instance of relatively LN velocity use and inspired the source scientist to begin developing the NI map enhancement. The 2nd and 3rd cases demonstrate a poor and a good example of results from artificial Nyquist data, respectively. The 4th through 10th cases are examples of real-time LN data that perform well with the enhanced 2DVDA. The last 2 cases illustrate persistent problems with LN velocities.

Several times, the authors mention strong shear when referencing cases. To clarify, this can have different meanings depending on the environmental context. The most likely type of strong shear in a LN situation exceeds the Nyquist velocity to the extent that true aliasing masks it, as mentioned in Section 4.2. In other situations, strong shear could also refer to a sharp change in speed and/or direction over a small change in height (i.e. 0.5 km). This tends to occur at the leading edge of frontal boundaries, where the air displaced by the boundary is beginning to ride over the top of it.

5.1 *KDVN 14 October 2017: The Original*

The first "low Nyquist" case was reported by the field on 14 October 2017 from site KDVN (Davenport/Quad Cities, IL). A squall line with strong winds and hail moved southeast across the area. The site used the lowest available PRF at the time, which had a Nyquist velocity of 21.4 m/s and an unambiguous range of 175 km. Figure 3 shows the type of dealiasing error seen during that case. The errors occurred along the leading edge of the squall line, where inflow was starting to ride over the outflow. This type of shear environment proves

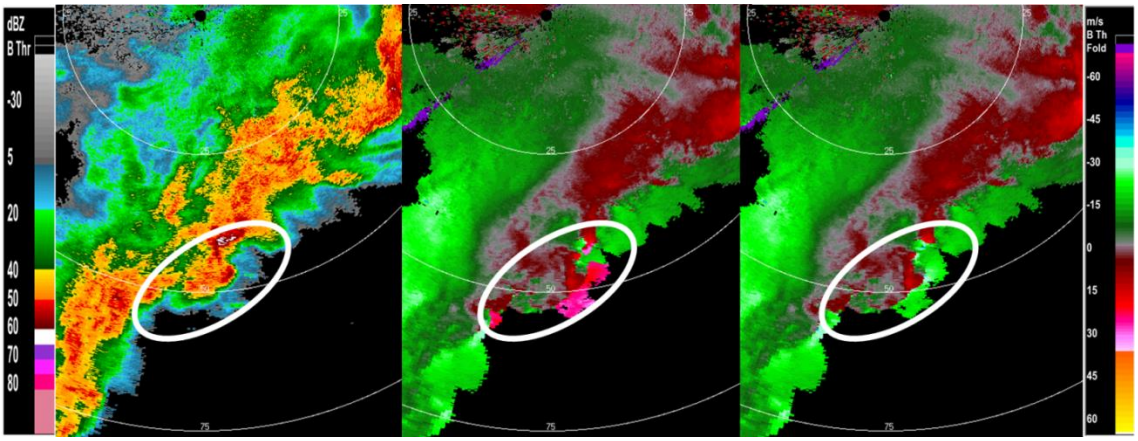

Figure 3: KDVN on 14 Oct 2017 at 22:58 UTC at elevation 0.5°. The middle image depicts the velocity dealiasing error as reported by the field, while the image on the right shows the corrected velocity generated by Build 19, both within the white circles. This type of shear has proven to be the most difficult to handle.

to be one of the most difficult situations for 2DVDA to handle. KDVN was one of the cases used for development of the NI map.

5.2 *Artificial Cases: KUDX and KFCX*

Both KUDX (Rapid City, SD) and KFCX (Roanoke, VA) were among the cases with "artificial" LN velocities. For the purposes of illustration, the KUDX case was chosen for its extremely poor performance in initial testing, while the KFCX case was chosen for its successful performance.

The KUDX data features an extremely strong mesocyclone moving east-southeast on 20 June 2015, and was chosen as an artificial Nyquist case specifically for the intensity of the winds. The site used a PRF with a Nyquist velocity of 27.3 m/s and an unambiguous range of 137 m. This was one of two cases undealiased and refolded with a Nyquist of 15 ms^{-1}. KOAX, the other 15 ms^{-1} case (not shown) showed similar dealiasing problems.

As shown by Figure 4, the initial results with the LN were not promising. The violent winds, peaking at least at 50 m/s, were potentially too strong for 2DVDA to unwrap with a 15 m/s Nyquist velocity. The error was carried azimuthally and radially, as can be seen in Figure 4B, due in part to an inherent weakness in 2DVDA's post-processing. This was discovered while testing Build 18 and rectified in Build 19. As it was, this case demonstrated an effective lower limit of 15 m/s early on and was used during the development of the NI map. Using the updated 2DVDA, KUDX now shows outstanding performance.

In contrast to KUDX, KFCX showed no dealiasing errors throughout testing. This case from 30 June 2012 featured a line of storms moving south-southeast. The original Nyquist velocity was 25.3 m/s, with an unambiguous range of 148 km. Below, Figure 5 shows an example from this case. Despite the strong winds, there were no dealiasing errors at the refolded Nyquist of 20 ms^{-1}. Why this case did not exhibit errors where similar cases did requires further analysis.

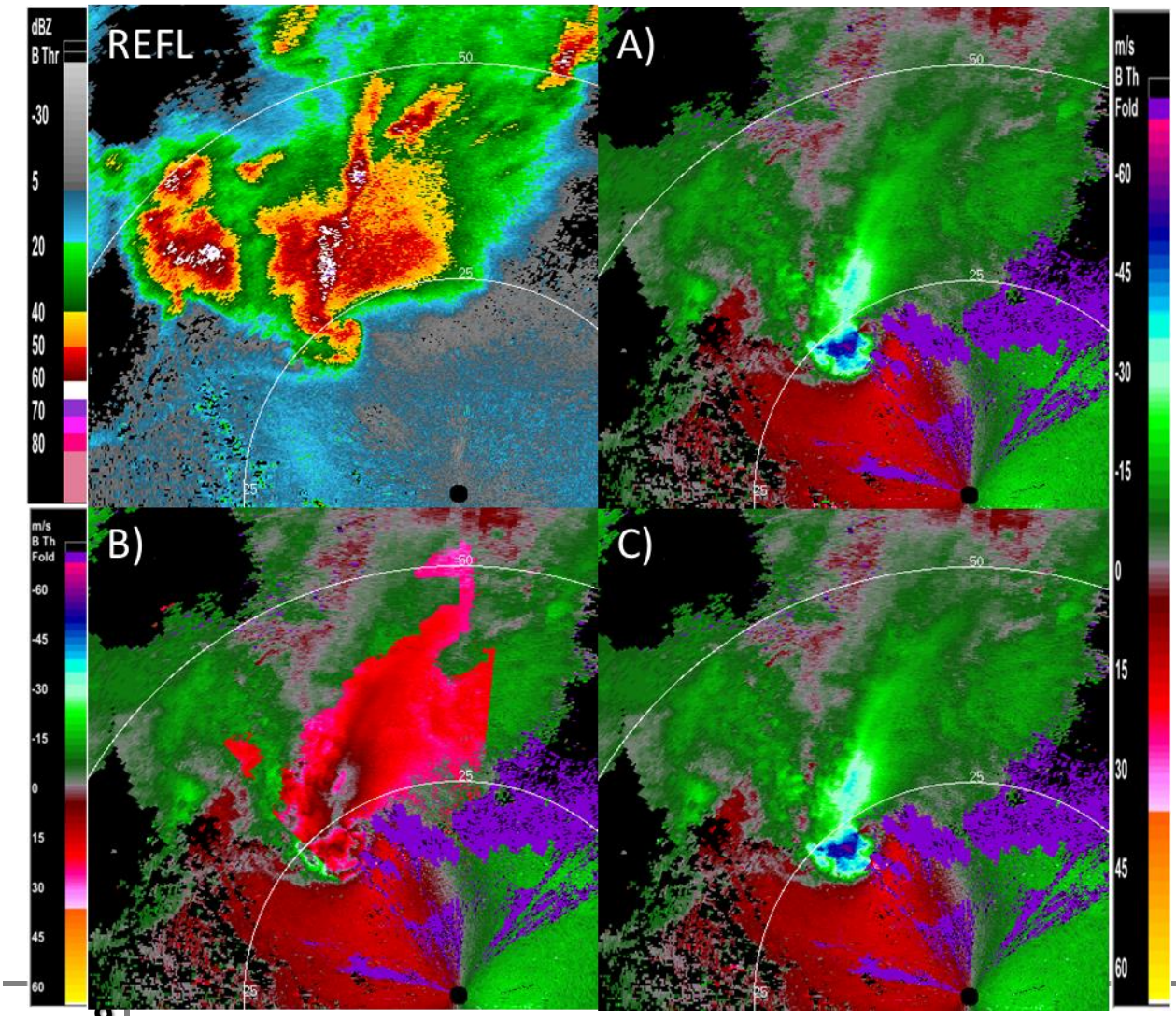

Figure 4: KUDX on 20 Jun 2015 at 02:47 UTC at elevation 0.5°. A) depicts the true data run with Build 18, which has no problems. B) shows the case undealiased and re-folded with Nyquist 15 m/s, again with Build 18. Note the large, erroneous swath of outbound velocities – this was one of the worst-performing cases. Finally, C) shows the field corrected with Build 19's updated 2DVDA. Reflectivity is provided for context.

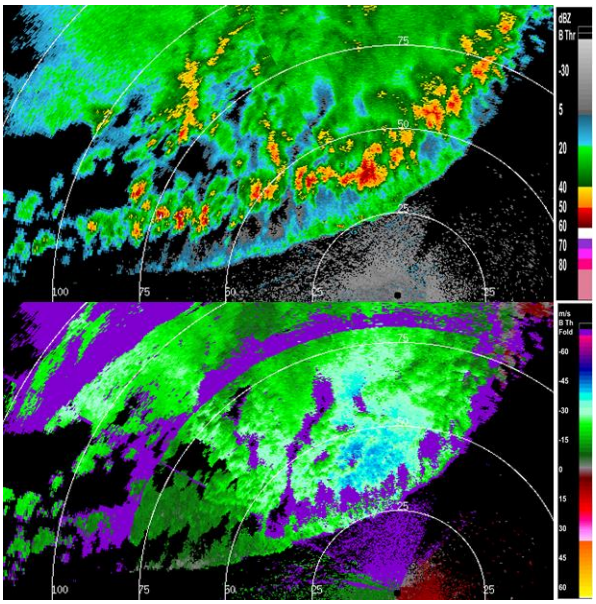

Figure 5: KFCX on 30 Jun 2012 at 00:43 UTC at elevation 0.5°. The velocity image was generated with Build 18 using an artificial Nyquist of 20 m/s and is identical to results from Build 19 at 20 m/s. The original Nyquist velocity was 25.3 m/s.

5.3 *KAMA 25 June 2018: The First PRF 2*

This case from Amarillo, TX represents the earliest of the Build 18 low PRF data sets. The weather for this case was complex, which added to the dealiasing difficulty. A broken line of storms drifted southeast, with at least 3 separate outflow boundaries moving more rapidly south and southeast toward the radar. The turbulence is evident in the velocity images in Figure 5 below, while the site was running PRF 2.

The site changed PRFs throughout the time period of the case; it ran in PRF 2 for nearly an hour, switched to PRF 4 for another hour, and then transitioned between PRF 4 and higher PRFs for the remaining hour. Serious dealiasing failures occurred during PRFs 2 and 4, the latter leading to the identification of a major weakness in 2DVDA's logic. Remote shear from noisy weak trip echo at far range could trigger a section of post-processing to redo its solution, introducing significant error to important 1st trip echo. The discovery of this weakness encouraged the authors to ensure 2DVDA's NI map enhancement was targeted for Build 19 rather than Build 20.

The nature of the problems in PRF 2 differed from those in PRF 4. The root of the errors seen during PRF 2 was likely the turbulence and outflow near the radar. The changing thermal gradients produced by these boundaries likely caused beam propagation problems, which increases ambiguity about which section of atmosphere is truly being sampled. This in turn increases ambiguity of the raw data, which increases the likelihood of incorrect interpretation by the algorithm. It is worth noting that while the enhancements to 2DVDA improved KAMA drastically, there remain certain, small errors, which can be seen in the B19 image in Figure 6.

5.4 *KLZK 20 February 2019: Shear close to the radar*

After KAMA and a few subsequent problematic PRF 2 cases, the authors began actively searching for instances where sites used PRF 2 to find more data to analyze. In this way, the KLZK case was found. For a multitude of reasons, it performed poorly in Build 18, though the field did not report it.

On 20 February 2019 at Little Rock, AK, precipitation moved northeast across Arkansas. West of the radar, stretching southwest to northeast, a convective line developed and moved along a boundary evident in velocity data. This boundary moves slowly east throughout the test period (04 to 06 UTC). Other isolated convection trained over the rest of the coverage area, becoming more linear over time. Directional shear was strong during the time period, as evidenced by the 00 UTC and 12 UTC soundings and upper air observations (not shown), as well as by surface observations throughout the day.

Shear is often a difficult problem to handle, and Build 18's 2DVDA did not do well, as mentioned. Figure 7 below shows an example of the dealiasing problems characteristic of this case, as well as Build 19's improved dealiasing solution. Some of the errors in the B18 image in Figure 7 are due to the weakness discussed in Section 5.3, with KAMA.

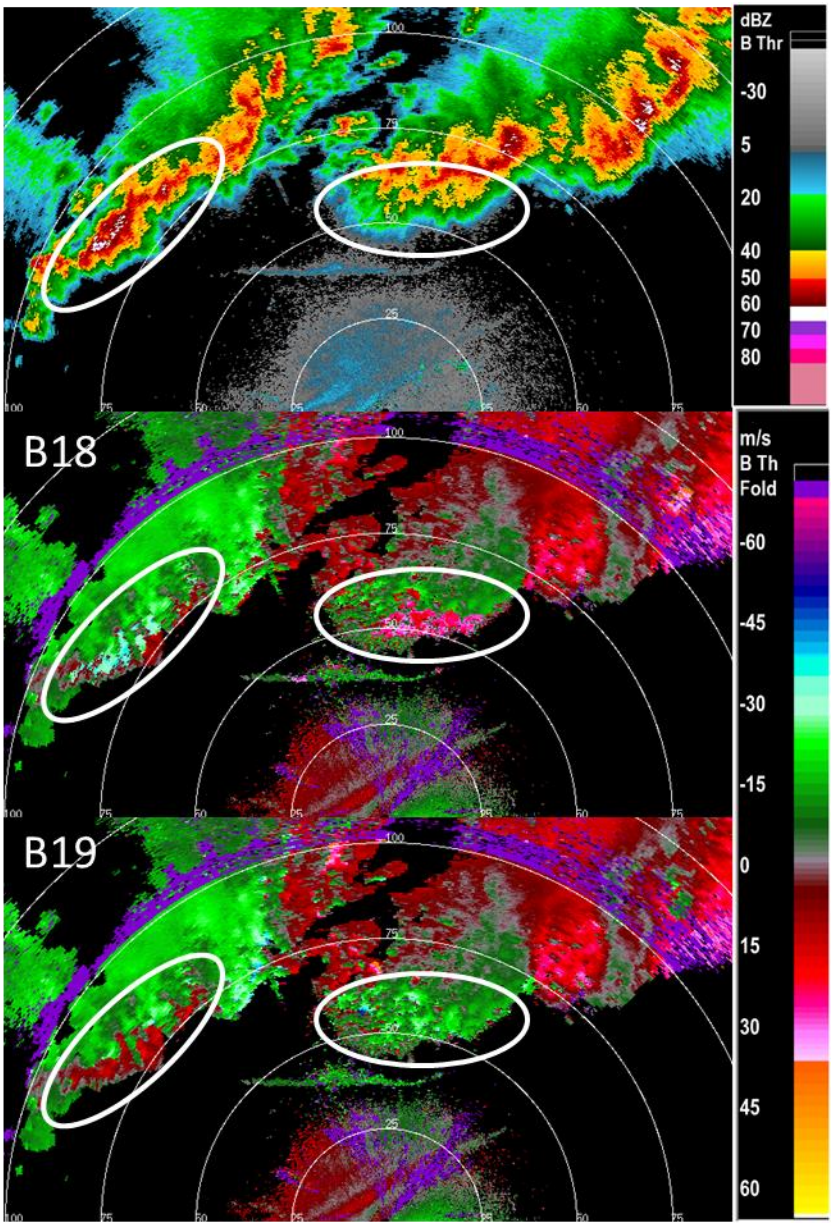

Figure 6: KAMA on 25 Jun 2018 at 03:45 UTC at elevation 0.5° (SAILS 2). The radar is at the bottom center of the image. Reflectivity (top) shows the outflow boundaries. The middle image is Build 18's velocity solution as seen by forecasters. The bottom image shows Build 19's solution, which is much cleaner. Note the errors within the white ovals in Build 18, while Build 19 has corrected the errors. The ovals were placed in the reflectivity image to give context to the velocity errors.

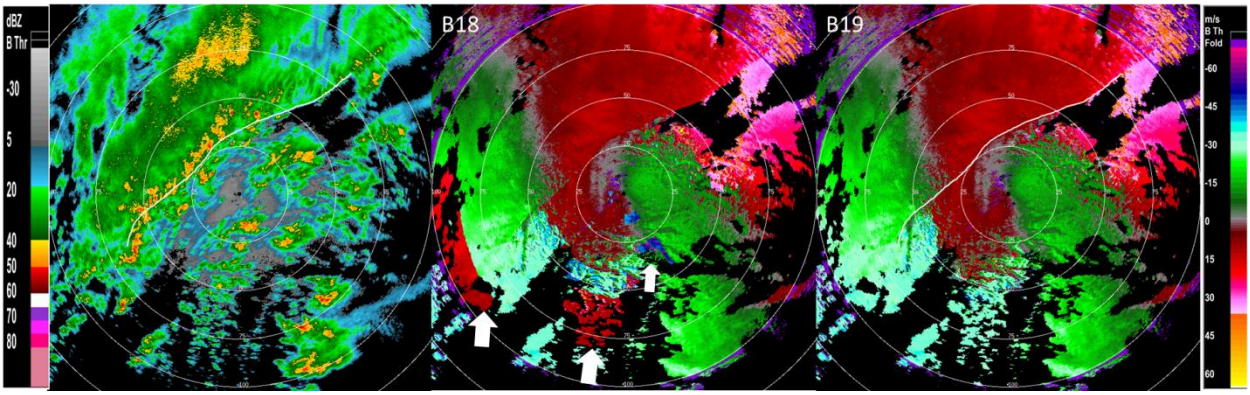

Figure 7: KLZK on 20 Feb 2019 at 04:05 UTC at elevation 0.5°. The precipitation is moving from southwest to northeast en masse; however, note the white line drawn on the reflectivity (left) and B19 velocity (right) images. This line denotes the boundary mentioned above. The line was not drawn in the B18 image to prevent detracting attention from the dealiasing errors and also so the reader can view the boundary cleanly. In the middle image, note the sector of erroneous velocities denoted by the white arrows. Build 19's 2DVDA, in contrast, gives a cleaner solution overall.

5.5 *13 March 2019 – The Good Trio*

One of the success stories of 2DVDA and PRF 2 occurred on 13 March 2019. While searching for PRF 2 cases, the authors discovered that three different, nearby sites – KLBB (Lubbock, TX), KFDR (Frederick, OK), and KTLX (Twin Lakes, OK) – used PRF 2 on the same day while precipitation associated with a frontal boundary approached or passed through the area (Figure 8).

Especially at KLBB, where the convection is strong and linear, the authors expected to see dealiasing errors, especially at far range. It is probable that the wind shear is not strong enough to give 2DVDA trouble.

5.6 *KRAX 14 September 2018 – Hurricane Florence*

Another success story occurred over the course of Hurricane Florence, in mid-September 2018. The 2DVDA has had problems with strong hurricanes at a distance in the recent past, but it performed quite well here. KRAX (Raleigh, NC) captured the entirety of the hurricane with PRF 2 over a 4-day period. The authors ran 5 hours from 14 September, when Florence was coming onshore. The only notable dealiasing error during that time occurs when the site transitions from a higher PRF; the range folding shifts further from the radar and because 2DVDA has no history for the newly available data, it dealiases that wedge incorrectly. This lasts for only one volume before it corrects itself. Figure 9 below shows an image from Build 18; Build 19 is functionally identical (not shown).

5.7 *30 June 2019 KDLH – Shear Example*

This case represents one of the remaining issues with low PRFs and 2DVDA – strong shear. Almost every egregious error during initial testing involved strong shear cases. Even the enhanced 2DVDA in Build 19 still has problems with strong shear.

The KDLH (Duluth, MN) case exemplifies the difficulties with strong shear at leading edge of a boundary. Again, the case features a strong line of storms. Moving quickly southeast, the main line has gone well past the radar by the start of the case period at 11 UTC. See Figure 10 below.

5.8 *21 June 2019 KEAX – Range Example*

Potentially the most difficult of problems to correct for is the raw data ambiguity caused by beam broadening at range. The sample volume has expanded to the point where it becomes difficult to determine what part of the atmosphere the data are coming from. This becomes more of an issue during turbulent weather, when the beam propagation path can vary, so this often goes hand-in-hand with errors related to strong shear.

This case, KEAX in Pleasant Hill, MO features two successive squall lines approaching the radar from the west. The time frame of the case ranges from just after the first, stronger squall line passes the radar to just before the second line hits. Figure 11 captures one of these moments.

This case provides an excellent illustration of the difficulties with interpreting shear and weak signal at far range. At 0.5°, there is a zero-isodop that is probably real. At 1.3°, what data exist in that area are weak outbound. Somewhere between these two elevation scans, there is a transition, and at this range, the beam height and sample volume have increased enough that pinpointing exactly what's going on in that area at 0.9° is challenging.

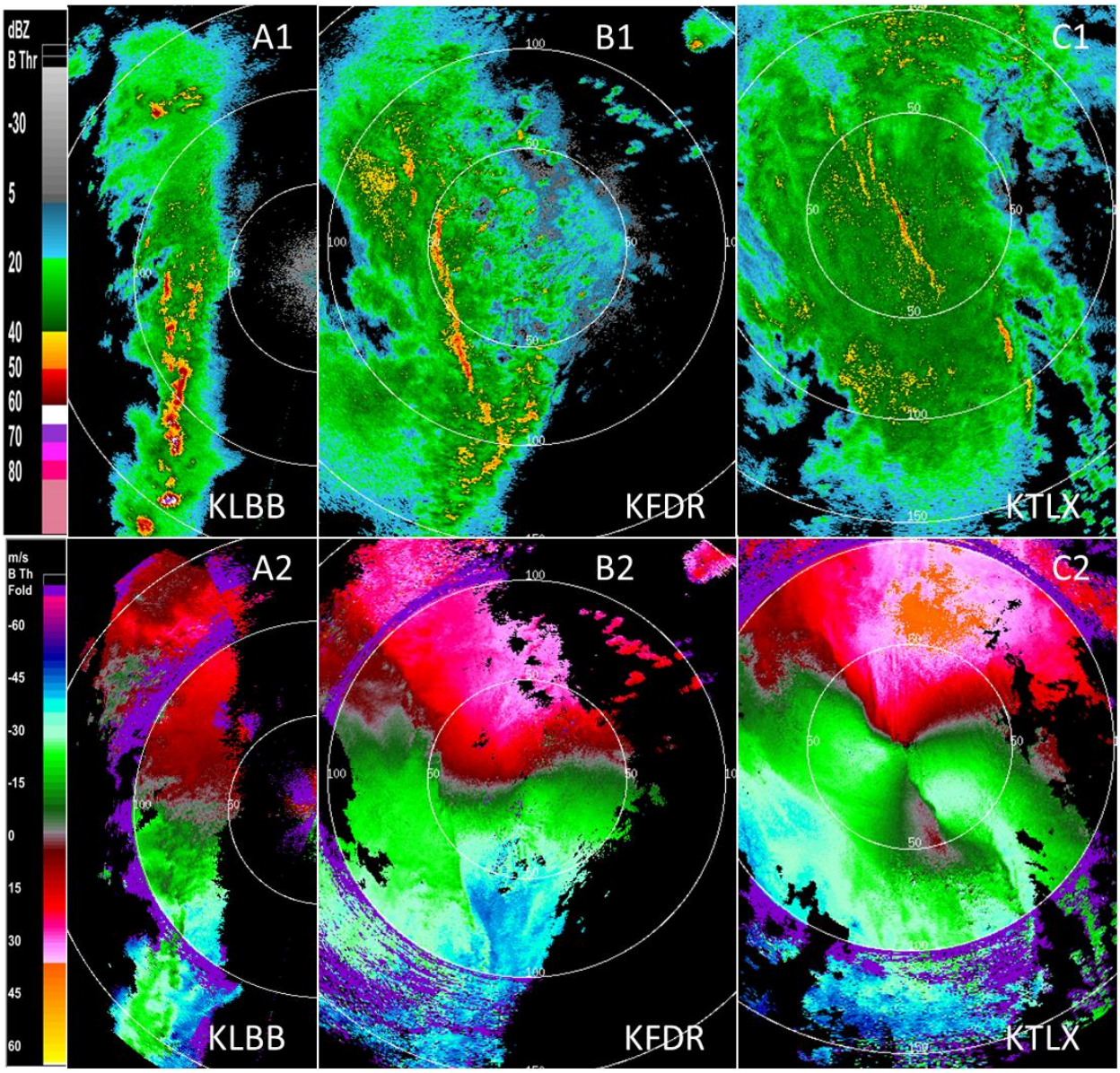

Figure 8: 13 Mar 2019, all at elevation 0.5°. Images A1 and A2 are from KLBB at 01:29 UTC; images B1 and B2 are from KFDR at 06:49 UTC; images C1 and C2 are from KTLX at 11:04 UTC. All images are from Build 18 as seen by the field; no dealiasing errors are evident and Build 19 is the same.

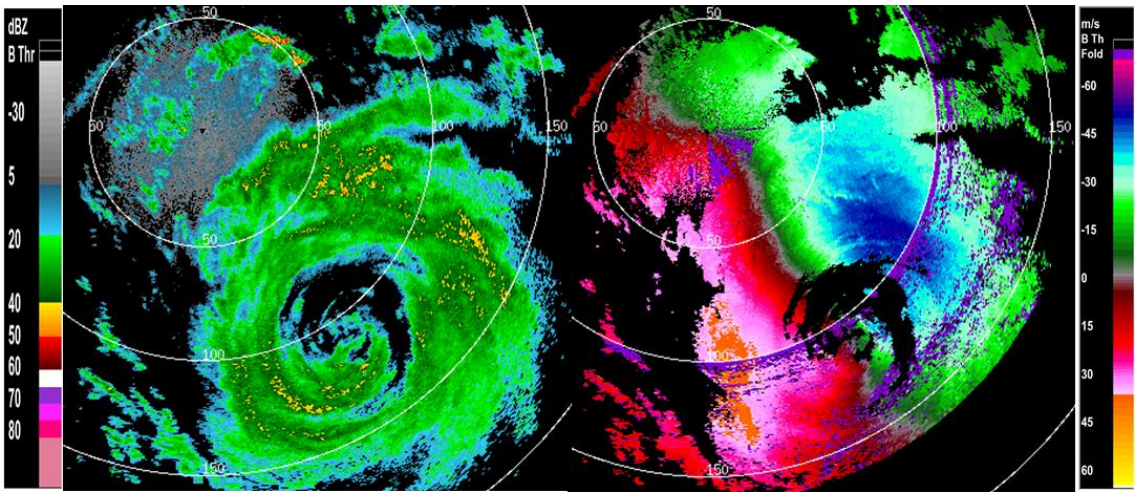

Figure 9: KRAX on 14 Sept 2019 at 06:53 UTC at elevation 0.5° (SAILS 3). Despite the amount of data beyond first trip of PRF 2, dealiasing errors are not present.

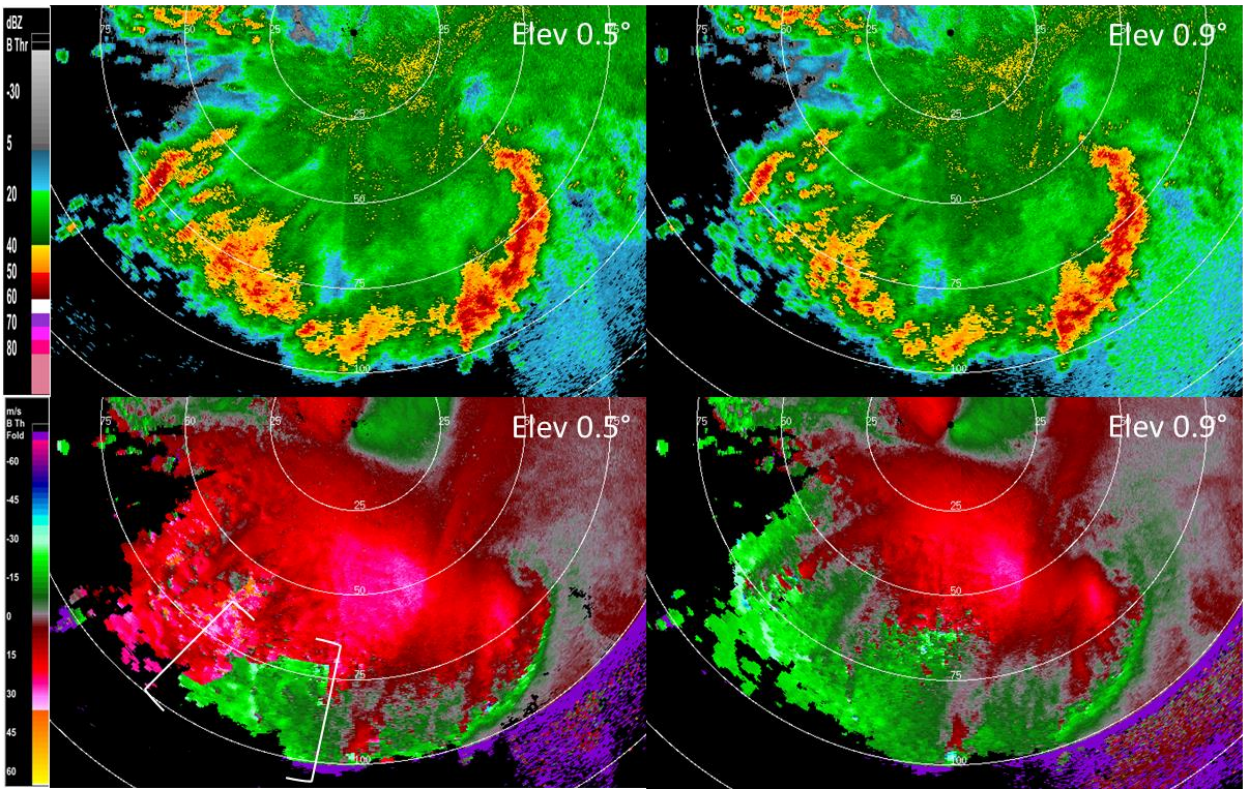

Figure 10: KDLH on 30 Jun 2019 at 11:52 UTC at elevations 0.5° and 0.9°. Overall, the weather is moving southeast. Note the error within the bracket in the bottom left velocity image. When compared to the corresponding area at elevation 0.9°, it is easier to see why dealiasing at 0.5° has difficulty. The directional shear between these two elevations is difficult to solve.

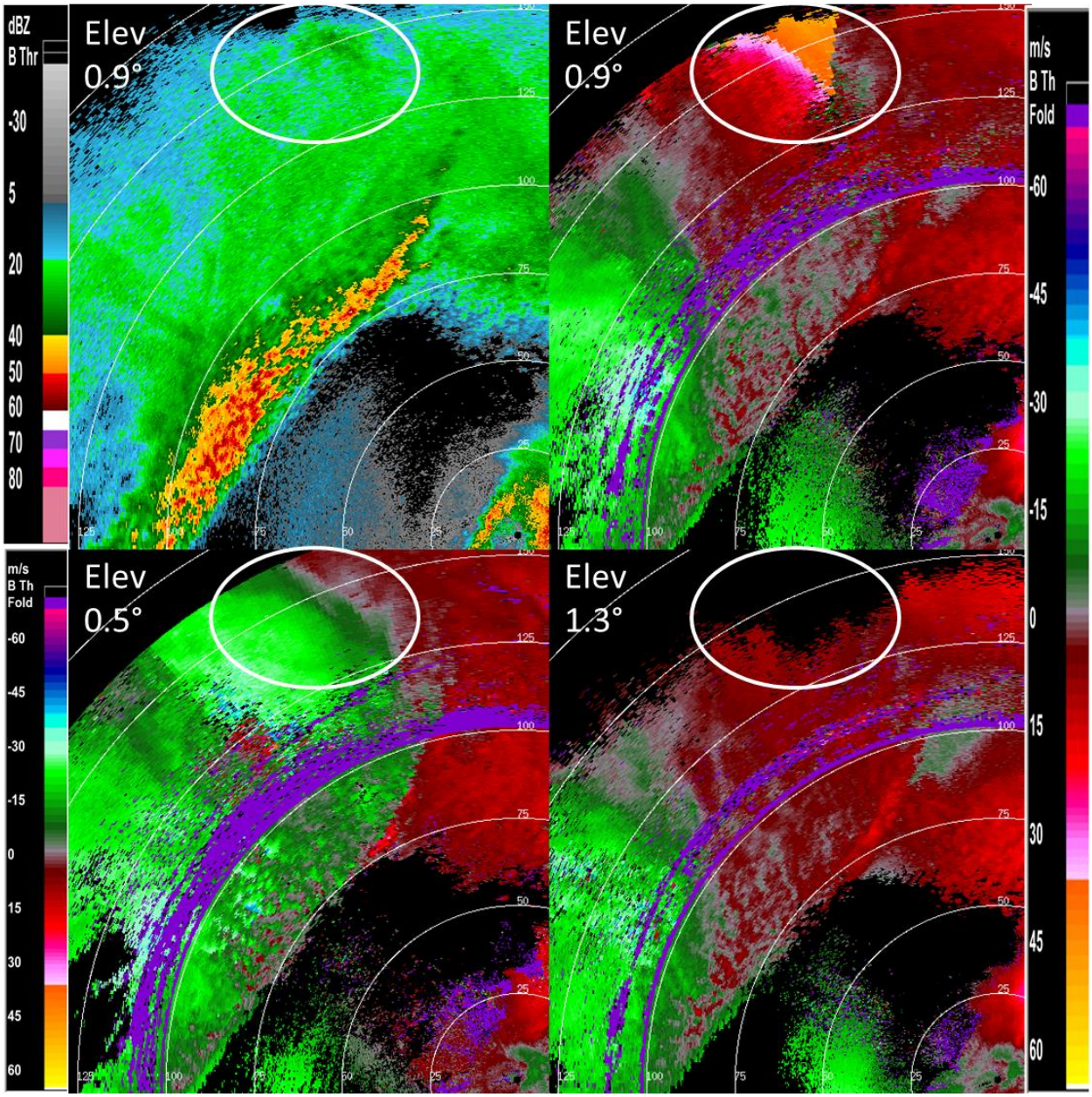

Figure 11: KEAX on 21 June 2019 at 13:41 UTC at elevation 0.9°. This is Build 19; Build 18 is not shown because its errors occur for similar reasons. The southwestern end of the first bow echo is visible near the radar, especially in reflectivity. Note the wedge of strong outbound at the top of the velocity image, circled in white, and the corresponding weak signal in the reflectivity. The elevations surrounding 0.9° have been included for additional context. Note the inbound velocities in the white circle at 0.5° and the mostly echoless white circle in 1.3°. This uncertain data is part of the difficulty with this case.

6. CONCLUSIONS AND FUTURE WORK

It is a desired goal of weather radars such as the WSR-88D to reduce range ambiguity as much as possible while maintaining a balance of interpretable velocities free of error. Using LN velocities is one method of reducing range ambiguity. Results in this study show that the WSR-88D's default dealiasing scheme, 2DVDA, has success with LNs down to 20 ms^{-1} for most weather cases. Cases with strong shear are persistently challenging to dealias at LNs, especially when the shear is near or beyond the first trip boundary of PRF 2 at 187 km and the vertical shear discontinuity is contained entirely within the beam.

With the NI map enhancement, errors due to horizontal discontinuities near the Nyquist co-interval are largely eliminated. The overall success rate of the enhanced 2DVDA to be fielded in Build 19 shows that using low Nyquist velocities is a viable strategy to improve Doppler coverage.

The authors would like to further explore the mechanisms that determine why failures occur for some cases and not for other, similar cases. Naturally, part of the goal of such investigation would be to identify areas in 2DVDA that can be further improved. The other end goal would be to define a set of conditions that could help predict when dealiasing problems at low PRFs would be most likely. When these conditions are met, the use of a higher PRF would be recommended, either via a message to the user or invoked automatically by the PRF selection algorithm.

7. ACKNOWLEDGEMENTS

The authors would like to thank their ROC Engineering and ROC Data Quality colleagues who provided expertise and knowledge during the testing process, as well as for their feedback for the paper.

8. REFERENCES

Conway, J.W. K.D. Hondl, and M.D. Eilts, 1997: Minimizing the Doppler Dilemma using a unique redundant scanning strategy and multiple pulse repetition frequency dealiasing algorithm. *Preprints: 28th Conf. on Radar Meteor,* Austin, TX, AMS, 315-316.

Jing, Z. and G. Wiener, 1993: Two-Dimensional Dealiasing of Doppler Velocities. *J. Atmos. Oceanic Technol.*, **10**, 798-808

Losey, A., W. D. Zittel, and Z. Jing, 2017: Use of Mid-Level Model Data and VAD Winds to Improve WSR-88D Velocity Dealiasing. *Extended Abstracts, 38th Conf. on Radar Meteor.,* Chicago, IL, USA, AMS. Available Online at: https://ams.confex.com/ams/38RADAR/meetingapp.cgi/Person/179846.

Sachidananda, M., D. Zrnić, R. J. Doviak, and S. Torres, 1998: Signal Design and Processing
Techniques for WSR-88D Ambiguity Resolution, Part 2

Saxion, D. S., R. D. Rhoton, R. L. Ice, G. T. McGehee, D. A. Warde, O. E. Boydstun, W. D. Zittel, S.
Torres, G. Meymaris, 2007: New Science for the WSR-88D: Implementing a Major Mode On the SIGMET RVP8, 23rd International Conference on Interactive Information Processing Systems for Meteorology, Oceanography, and Hydrology.

Torres, S., 2006: Range and velocity ambiguity mitigation on the WSR-88D: Performance of the staggered PRT algorithm. *Extended Abstracts, 22nd International Conference on Interactive Information Processing Systems for Meteorology, Oceanography, and Hydrology*, Atlanta, GA, USA, AMS, 9.9. Available online at: http://cimms.ou.edu/rvamb/Documents/AMS_IIPS_2006.pdf.

Zittel, W. D and Z. Jing, 2012: Comparison of a 2-D velocity dealiasing algorithm to the legacy WSR-88D velocity dealiasing algorithm during Hurricane Irene. *30th Conf. on Hurricanes and Tropical Meteorology,* Jacksonville/Ponte Vedra, FL, AMS, 7C.7.